Observation of a Pseudoscalar State in $J/\psi \rightarrow \gamma\phi\phi$ near $\phi\phi$ Threshold

Z. Bai, G. T. Blaylock, T. Bolton, T. E. Browder, J. S. Brown, K. O. Bunnell, T. H. Burnett, R. E. Cassell, D. Coffman, V. Cook, F. DeJongh, D. E. Dorfan, J. Drinkard, G. P. Dubois, G. Eigen, K. F. Einsweiler, B. I. Eisenstein, T. Freese, C. Gatto, G. Gladding, J. Hauser, C. A. Heusch, D. G. Hitlin, J. M. Izen, P. C. Kim, J. Labs, A. Li, W. S. Lockman, U. Mallik, C. G. Matthews, A. I. Mincer, R. Mir, P. M. Mockett, R. F. Mozley, B. Nemati, A. Odian, L. Parrish, R. Partridge, D. Pitman, S. A. Plaetzer, J. D. Richman, H. F. W. Sadrozinski, M. Scarlatella, T. L. Schalk, R. H. Schindler, A. Seiden, C. Simopoulos, I. E. Stockdale, W. Toki, B. Tripsas, F. Villa, M. Z. Wang, S. Wasserbaech, A. J. Weinstein, S. Weseler, H. J. Willutzki, D. Wisinski, W. J. Wisniewski, R. Xu, and Y. Zhu

(The Mark III Collaboration)

California Institute of Technology, Pasadena, California 91125
University of California at Santa Cruz, Santa Cruz, California 95064
University of Illinois at Urbana-Champaign, Urbana, Illinois 61801
University of Iowa, Iowa City, Iowa 52242
Stanford Linear Accelerator Center, Stanford, California 94309
University of Washington, Seattle, Washington 98195
(Received 1 March 1990)

We present a study of the radiative decay $J/\psi \rightarrow \gamma\phi\phi$ in the $\gamma K^+K^-K^+K^-$ and $\gamma K^+K^-K_S^0K_L^0$ final states. A pseudoscalar state is observed in the $\phi\phi$ invariant-mass spectrum at 2.22 GeV/c^2 with a width of 150 MeV/c^2. The product branching ratios are $B(J/\psi \rightarrow \gamma X)B(X \rightarrow \phi\phi) = (3.3 \pm 0.8 \pm 0.5) \times 10^{-4}$ for the $\gamma K^+K^-K^+K^-$ mode and $B(J/\psi \rightarrow \gamma X)B(X \rightarrow \phi\phi) = (2.7 \pm 0.6 \pm 0.6) \times 10^{-4}$ for the $\gamma K^+K^-K_S^0K_L^0$ mode. No evidence for 2^{++} states below 2.4 GeV/c^2 is found in this decay.

PACS numbers: 14.40.Cs, 13.40.Hq

Interest has focused recently on the $\phi\phi$ system produced in radiative J/ψ decays, since this process may produce glueballs, hybrids, or four-quark states.[1] Structures in the $\phi\phi$ invariant-mass spectrum have been observed by several experiments in the reaction $\pi^-p \rightarrow \phi\phi n$.[2] One group, after performing a partial-wave analysis, has resolved three broad 2^{++} resonances near $\phi\phi$ threshold. These states have been claimed to be glueballs,[3] since the production process is Okubo-Iizuka-Zweig (OZI) suppressed. If this hypothesis is correct, these states should also be produced in radiative J/ψ decays.[1] The DM2 group[4] has reported the observation of a low-mass enhancement in $J/\psi \rightarrow \gamma\phi\phi$ at 2.25 GeV/c^2 with a preferred spin-parity of $J^P = 0^-$. Other pseudoscalar states near threshold as well as at higher mass have been observed[5] in radiative J/ψ decays to $\rho\rho$ and $\omega\omega$; the $\eta(2100)$ is the only state kinematically accessible to $\gamma\phi\phi$. We present herein a study of $J/\psi \rightarrow \gamma\phi\phi$ in the $\gamma K^+K^-K^+K^-$ and $\gamma K^+K^-K_S^0K_L^0$ final states,[6] using 4.9×10^6 produced J/ψ events recorded with the Mark III detector[7] at the SLAC e^+e^- storage ring SPEAR.

The study of the $\gamma K^+K^-K^+K^-$ channel is made difficult by kaon decays which severely affect the detection efficiency, especially at low $\phi\phi$ masses ($m_{\phi\phi}$), where kaon momenta are smallest. For $m_{\phi\phi}$ below 2.4 GeV/c^2, 60% of all events with four observed charged tracks suffer from momentum mismeasurements because of track kinks due to decays in flight. A four-constraint (4C) kinematic fit by the hypothesis $J/\psi \rightarrow \gamma K^+K^-K^+K^-$ typically fails for these events. A substantial increase in detection efficiency can be obtained with 1C kinematic fits by the hypothesis $J/\psi \rightarrow \gamma K^+K^-K^\pm(K^\mp_{\text{miss}})$, where the most poorly measured track is excluded from the fit. To ensure a consistent procedure for events with four well-measured tracks, a 1C fit is performed to all three-track combinations by omitting one track at a time, retaining the fit with the lowest χ^2. In events with several isolated photon candidates,[8] the radiative photon is always chosen to be the shower closest to the direction of the missing momentum of the four charged tracks. Candidates are selected from events which have the following: at least two well-identified kaon tracks,[9] no pion candidate[9] (unless two like-sign kaons are found), a 1C-fit probability greater than 2%, and less than five isolated photons.

Figure 1(a) shows a scatter plot of the invariant masses $m_{K^+K^-}$ vs $m_{K^\pm K^\mp_{\text{miss}}}$. A clear $\phi\phi$ signal is observed, providing evidence for the process $J/\psi \rightarrow \gamma\phi\phi$, since the modes $J/\psi \rightarrow \phi\phi$ and $J/\psi \rightarrow \phi\phi\pi^0$ are forbidden by C invariance. The final $\phi\phi$ sample is extracted by requiring $|m_{K\bar{K}} - m_\phi| \leq 3\sigma$, where the measured resolutions are $\sigma_{K^+K^-} = 3.8$ MeV/c^2 and $\sigma_{K\bar{K}_{\text{miss}}} = 5.9$ MeV/c^2. The resulting $\phi\phi$ invariant-mass spectrum for the 1C-fit events, shown in Fig. 2(a), contains a total of 168 events. The mass resolution, determined by Monte Carlo simulation, varies from 12 MeV/c^2 at 2.2 GeV/c^2 to 19 MeV/c^2 in the η_c region. Potential background sources consist of modes such as $\gamma\phi\phi + n\pi^0$'s, $\gamma\phi K^+K^-$, ϕK^+K^-, $\gamma\phi K^+K^-\pi^0$, $\phi K^+K^-\pi^0$, and $K^+K^-\pi^+\pi^- + n\gamma$. While the channels $\gamma\phi\phi + n\pi^0$'s are found to be negligible, the contribution of the other backgrounds is estimated from the events inside the lightly shaded areas

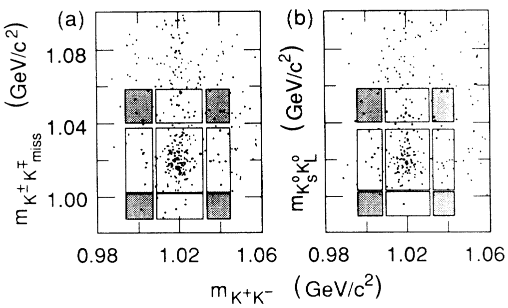

FIG. 1. Scatter plots for $J/\psi \to \gamma 4K$: (a) $m_{K^+K^-}$ vs $m_{K^{\pm}K^{\mp}_{\text{miss}}}$, plotting only the combination closest to the $\phi\phi$ overlap region; (b) $m_{K^+K^-}$ vs $m_{K_S^0K_L^0}$. Events in the shaded regions are used for background estimates.

in Fig. 1(a), after subtracting the contribution from the darkly shaded areas and correcting for feedthrough from real $\gamma\phi\phi$ events as determined from a Monte Carlo simulation. The non-$\phi\phi$ background, amounting to 9%, is uniform in $m_{\phi\phi}$.

Figure 2(c) shows the $\phi\phi$ invariant-mass spectrum after efficiency correction. A prominent structure around 2.2 GeV/c^2 is visible, as is the η_c. The mass spectrum is fitted by a relativistic p-wave Breit-Wigner line shape with a mass-dependent width[10] but without a form factor, a nonrelativistic Breit-Wigner line shape for the η_c, a uniform background, and three-body phase space. Table I summarizes the results. For the low-mass state, the mass, width, and product branching ratio are $M = 2230 \pm 25 \pm 15$ MeV/c^2, $\Gamma = 150^{+300}_{-60} \pm 60$ MeV/c^2, and $B(J/\psi \to \gamma X)B(X \to \phi\phi) = (3.3 \pm 0.8 \pm 0.5) \times 10^{-4}$. The systematic errors include uncertainties in the luminosity measurement, event selection, background subtraction, efficiency determination, and different fit functions of the $\phi\phi$ spectrum. We have also made fits which include a production and decay form factor using both Blatt-Weisskopf and Gaussian shapes. A dispersion relation was used,[11] to ensure a proper form-factor cutoff at infinity. Within errors, the mass and width remain the same, but the branching ratio increases by up to a factor of 2, as the fit attempts to accommodate the cluster of events around 2.5 GeV.[12] This is not, however, a realistic description, since the events around 2.5 GeV are not $J^P = 0^-$ (see below). For the η_c, the mass and width are in good agreement with nominal values;[13] the product branching ratio is consistent with the previous Mark III result, which was based on the first half of the data sample.[14] The total branching ratio for radiative $\phi\phi$ production is $B(J/\psi \to \gamma\phi\phi) = (7.5 \pm 0.6 \pm 1.2) \times 10^{-4}$.

There are 80 events which have satisfactory 4C kinematic fits by the $\gamma K^+K^-K^+K^-$ hypothesis. Because of the small detection efficiency at low $m_{\phi\phi}$ the η_c is the only significant signal observed in the $\phi\phi$ mass spectrum. The events in the low-mass region, however, are consistent with the signal events in the 1C fit. The η_c mass so obtained, $2969 \pm 4 \pm 4$ MeV/c^2, and the product branching ratio, $B(J/\psi \to \gamma\eta_c)B(\eta_c \to \phi\phi) = (9.4 \pm 2.3 \pm 1.6) \times 10^{-5}$, agree well with the results from the 1C fit.

Since the K_L detection efficiency is low and difficult to determine, K_L detection is not required in the $\gamma K^+K^-K_S^0K_L^0$ channel. Candidates are instead selected by 1C kinematic fits by the hypothesis $J/\psi \to \gamma K^+K^-\pi^+\pi^-(K_L^0)_{\text{miss}}$, identifying kaons and pions by time of flight and dE/dx. If several kaon- or pion-pair combinations exist, we choose that which best matches a ϕ or a K_S^0. All isolated showers are considered as candidates for the radiative photon. Because of the poor photon-energy resolution, the χ^2 of the 1C fit does not alone provide a sufficient background rejection. The radiative photon is chosen to be that photon for which the quantity $\chi^2 + [(m_{K^+K^-} - m_\phi)/\sigma_{K^+K^-}]^2 + [(m_{K_S^0K_L^0} - m_\phi)/\sigma_{K_S^0K_L^0}]^2$ is minimal. In order to improve the $K_S^0K_L^0$ mass resolution, a 2C kinematic fit is performed by adding the K_S^0 constraint. Candidates are retained if the 2C-fit probability is greater than 1%, the event contains either two well-identified kaons or one well-identified kaon and two well-identified pions, and less than four isolated photons are present.

Figure 1(b) shows the scatter plot of $m_{K^+K^-}$ vs $m_{K_S^0K_L^0}$. A $\phi\phi$ enhancement is again visible. The $\phi\phi$ signal events are selected as above, using the measured resolutions of $\sigma_{K^+K^-} = 3.5$ MeV/c^2 and $\sigma_{K_S^0K_L^0} = 5.6$ MeV/c^2. The resulting $\phi\phi$ invariant-mass spectrum contains a total of 119 events [see Fig. 2(b)]. The $\phi\phi$ mass resolution varies from 13 MeV/c^2 at 2.2 GeV/c^2 to 30 MeV/c^2 at the η_c. In this case, the background contribution, estimated as above, originates from modes such as $\gamma\phi K^+K^-$, ϕK^+K^-, $\gamma\phi K^+K^-\pi^0$, and $\phi K^+K^-\pi^0$, with $\phi \to K_S^0K_L^0$,

TABLE I. Fit results for the $\phi\phi$ mass spectra from the $\gamma K^+K^-K^+K^-$ and $\gamma K^+K^-K_S^0K_L^0$ final states.

Final state	Mass (MeV)	Width (MeV)	$10^4 B(J/\psi \to \gamma X)B(X \to \phi\phi)$[a]
$\gamma K^+K^-K^+K^-$	$2230 \pm 25 \pm 15$	$150^{+300}_{-60} \pm 60$	$3.3 \pm 0.8 \pm 0.5$
$\gamma K^+K^-K_S^0K_L^0$	$2214 \pm 20 \pm 15$	150 fixed	$2.7 \pm 0.6 \pm 0.6$
$\gamma K^+K^-K^+K^-$	$2981 \pm 8 \pm 3$	10.3 fixed	$0.93 \pm 0.20 \pm 0.16$
$\gamma K^+K^-K_S^0K_L^0$	$2956 \pm 12 \pm 12$	10.3 fixed	$0.85 \pm 0.27 \pm 0.18$

[a]The systematic errors in the branching ratios include the following contributions which are added in quadrature: uncertainties in the luminosity measurement (8.5%), uncertainties from the event selection, background subtraction and efficiency determination (13% for $\gamma K^+K^-K^+K^-$ and 18% for $\gamma K^+K^-K_S^0K_L^0$), and uncertainties in the fit (6%).

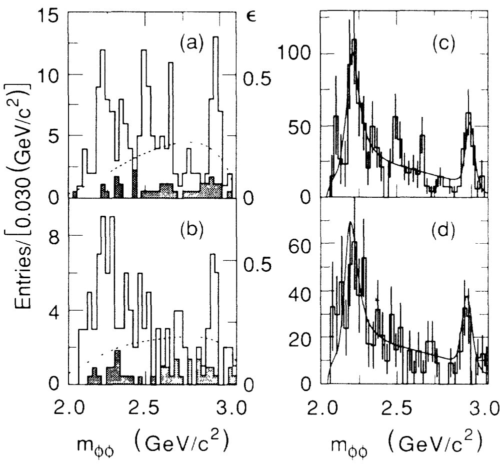

FIG. 2. The observed $\phi\phi$ invariant-mass spectra from (a) $J/\psi \to \gamma K^+K^-K^+K^-$ and (b) $J/\psi \to \gamma K^+K^-K_S^0K_L^0$; (c),(d) the corresponding $\phi\phi$ invariant-mass spectra after efficiency correction. Shaded histograms show background estimates; dashed curves show detection efficiencies denoted by ϵ; solid curves show fits described in the text.

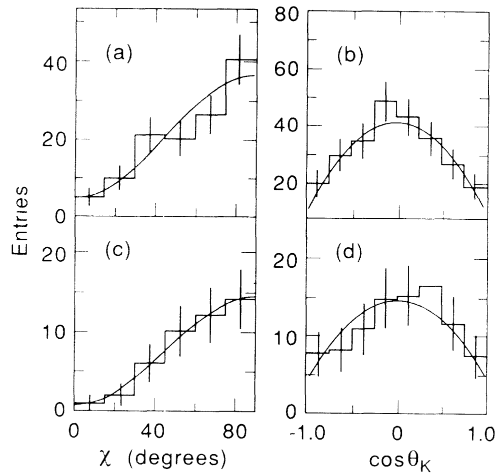

FIG. 3. Angular distributions for $J/\psi \to \gamma\phi\phi$ after efficiency correction for both modes combined: (a),(b) The χ and $\cos\theta_K$ distributions for the low-mass state (2.05–2.39 GeV/c^2); (c),(d) the χ and $\cos\theta_K$ distributions for η_c (2.92–3.04 GeV/c^2). The solid curves show fits described in the text.

and from events containing two kaons, two pions, and photons. The background (18%) is again uniform. The hadronic background $J/\psi \to \phi K_S^0 K_S^0$ with $K_S^0 \to \pi^0\pi^0$ and $\phi \to K^+K^-$ contributes at most one event in the region above 2.8 GeV/c^2.

Figure 2(d), showing $m_{\phi\phi}$ in the $\gamma K^+K^-K_S^0K_L^0$ mode after efficiency correction, confirms the $\gamma K^+K^-K^+K^-$ result. The spectrum is fitted with the same function used above. In order to obtain stable fits, it was necessary to fix the width of the low-mass Breit-Wigner linewidth to the value obtained in the $\gamma K^+K^-K^+K^-$ mode. The mass and product branching ratio for the low-mass state are $M = 2214 \pm 20 \pm 15$ MeV/c^2 and $B(J/\psi \to \gamma X)B(X \to \phi\phi) = (2.7 \pm 0.6 \pm 0.6) \times 10^{-4}$. The results, summarized in Table I, confirm those in $\gamma K^+K^-K^+K^-$.

The distributions of the angle between the ϕ decay planes in the $\phi\phi$ rest frame, χ, and the polar angle of the K^+ (or K_S^0) in its ϕ rest frame, θ_K, provide a spin-parity analyzer of states decaying into two vector mesons.[15] Including a non-$\phi\phi$-background term a, the angular distributions are given by

$$W(\chi) \propto a + (1-a)[1 + \beta\cos(2\chi)],$$

$$W(\cos\theta_K) \propto a + (1-a)[1 + \tfrac{1}{2}\zeta(3\cos^2\theta_K - 1)].$$

Both β and ζ are functions of the helicity amplitudes characterizing the spin-parity of the intermediate state decaying into $\phi\phi$. Thus a measurement of β determines the parity, since $0 \le P\beta \le 1$. For a pseudoscalar, $\beta = -1$ and $\zeta = -1$.

Figures 3(a) and 3(b) show the χ and $\cos\theta_K$ distributions between threshold and 2.40 GeV/c^2 after efficiency correction for both modes combined. While the efficiencies in χ and $\cos\theta_K$ for both pairs $K^\pm K^\mp_{\rm miss}$ and $K_S^0K_L^0$ are uniform, the $\cos\theta_K$ efficiency for the other K^+K^- pair drops near $|\cos\theta_K| = 1$ by 20%. The observed χ distributions peak at large angles, indicating $J^P = (\text{even})^-$. The $\cos\theta_K$ distributions exhibit a strong $\sin^2\theta_K$ dependence. A fit, using $W(\chi)$ and $W(\cos\theta_K)$ with $a = 0.11$,[16] yields $\beta = -0.85 \pm 0.11$ and $\zeta = -0.85 \pm 0.13$. This identifies the low-mass structure either as a pseudoscalar or as two interfering $J^P = 2^-$ ($L=1$, $S=1$ and $L=3$, $S=1$) states with nearly equal strength. The $L=3$ wave is, however, expected to be suppressed relative to the $L=1$ wave, especially near threshold. We therefore conclude that the low-mass structure is a pseudoscalar. To check the reliability of the technique, the χ and $\cos\theta_K$ distributions are examined in the η_c region ($2.90 \le m_{\phi\phi} \le 3.05$ GeV/c^2). The resulting distributions [Figs. 3(c) and 3(d)] are characteristic of a pseudoscalar. A fit with $a = 0.1$ yields $\beta = -1.0 \pm 0.2$ and $\zeta = -0.70 \pm 0.19$. The parameter β measured in 100-MeV/c^2 mass intervals is shown in Fig. 4. The pseudos-

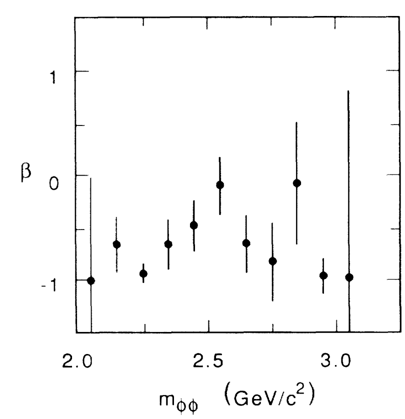

FIG. 4. The amplitude β as a function of $m_{\phi\phi}$.

TABLE II. Upper limits for g_T and $\xi(2230)$ production in $J/\psi \to \gamma\phi\phi$.

Mass region (GeV)	Number of events	β_p	$\epsilon_{\gamma K^+K^-K^+K^-}$	$\epsilon_{\gamma K^+K^-K_S^0K_L^0}$	$10^4 B(J/\psi \to \gamma X)B(X \to \phi\phi)$ (at 90% C.L.)
g_T (2.04–2.40)	122	0.29	0.12	0.14	< 1.16
$\xi(2230)$ (2.20–2.26)	32	0.39	0.12	0.15	< 0.38

calar component dominates below 2.4 GeV/c^2 and at the η_c.

In order to set a limit on $\xi(2230)$ and g_T production[17] in $J/\psi \to \gamma\phi\phi$, a maximum-likelihood fit is performed using $W(\chi)$. Assuming that, in addition to a pseudoscalar, partial waves with positive parity are present, the fraction of the $P=+1$ components is given by $f=(1-a)(1+\beta)/(1+\beta_p)$, where β_p is the average amplitude for the $P=+1$ components and β is the limit determined by integrating the log likelihood over the 90%-confidence-level interval. Because of unknown phases and relative fractions for the three g_T states, a determination of β_p is not possible. We therefore assume $\beta_p=0$, which yields the most conservative limit. The resulting upper limits for g_T and $\xi(2230)$ production presented in Table II are obtained by multiplying the observed number of events by f and normalizing the result to the total number of produced J/ψ events after correcting for the detection efficiencies and ϕ-decay branching ratios. The limit is a factor of 8 higher than a model-dependent prediction for g_T production in radiative J/ψ decays.[18]

In summary, we have observed a pseudoscalar state about 0.15 GeV/c^2 above $\phi\phi$ threshold in the radiative decay $J/\psi \to \gamma\phi\phi$ in two decay channels. This state may correspond to the 200-MeV/c^2-wide pseudoscalar state $\eta(2100)$ seen in $J/\psi \to \gamma\rho\rho$ at 2.138 GeV/c^2.[12] Additional pseudoscalars have also been seen in $J/\psi \to \gamma\rho\rho$ and $J/\psi \to \gamma\omega\omega$. The nature of these pseudoscalars is not presently understood. Possibilities include the second and third radial excitations of the pseudoscalar mesons[19] and well as $q\bar{q}g$ hybrids[20] or $qq\bar{q}\bar{q}$ states.[21]

We gratefully acknowledge the dedicated efforts of the SPEAR staff. One of us (G.E.) wishes to thank the Alexander von Humboldt Foundation for support. This work was supported in part by the U.S. Department of Energy, under Contracts No. DE-AC03-76SF00515, No. DE-AC02-76ER01195, No. DE-AC02-87ER40318, No. DE-AC03-81ER40050, and No. DE-AM03-76SF0034, and by the National Science Foundation.

[1]See references given in G. Eigen, in *Spectroscopy of Light and Heavy Quarks*, edited by U. Gastaldi, R. Klapisch, and F. Close, Ettore Majorana International Science Series Vol. 37 (Plenum, New York, 1989).

[2]A. Etkin *et al.*, Phys. Lett. B **201**, 568 (1988), and references therein; C. Daum *et al.*, Phys. Lett. **104B**, 246 (1981); T. F. Davenport *et al.*, Phys. Rev. D **33**, 2519 (1986); P. S. L. Booth *et al.*, Nucl. Phys. **B273**, 677 (1986).

[3]S. J. Lindenbaum and R. S. Longacre, Phys. Lett. **165B**, 202 (1985).

[4]D. Bisello *et al.*, Phys. Lett. B **179**, 294 (1986).

[5]D. L. Burke *et al.*, Phys. Rev. Lett. **49**, 632 (1982); R. M. Baltrusaitis *et al.*, Phys. Rev. D **33**, 1222 (1986); M. Bisello *et al.*, Phys. Rev. D **39**, 701 (1989); R. M. Baltrusaitis *et al.*, Phys. Rev. Lett. **55**, 1723 (1985).

[6]An earlier analysis of these final states is given in B. Tripsas, Ph.D. thesis, University of Illinois at Urbana Champaign, 1988 (unpublished).

[7]D. Bernstein *et al.*, Nucl. Instrum. Methods Phys. Res. **226**, 302 (1984).

[8]Isolated photons are showers of at least 40 MeV, which begin within the first seven radiation lengths of the sampling calorimeter (nine layers), contain at least two layers, and lie outside a 20° cone around each charged track.

[9]We use time of flight (TOF) for particle identification; dE/dx is used only if TOF is not available. A K is well identified if the measured TOF is within 4 s.d. of the K prediction and favors the K over the π hypothesis or if dE/dx provides a >4 s.d. K/π separation. A pion candidate is any track with a measured TOF (dE/dx) being consistent with a π hypothesis within 5 (4) s.d.

[10]J. D. Jackson, Nuovo Cimento **34**, 1644 (1964). Bose-Einstein correlations are negligible; the ϕ is narrow and K^+K^- pair selection is largely unambiguous.

[11]N. Törnqvist, Acta Phys. Pol. B **16**, 503 (1984); (private communication).

[12]We have also tested the hypothesis that the low-mass $\phi\phi$ state is actually the $\eta(2100)$ observed in $\gamma\rho\rho$. Were we to assume the $\eta(2100)$ decays dominantly to channels other than $\phi\phi$, the total width would be independent of the $\phi\phi$ kinematics. For the $\gamma K^+K^-K^+K^-$ channel a fit to the data in Fig. 1(c) with a constant total width yields a mass $M=2196\pm20$ MeV/c^2 and a width $\Gamma=110\pm50$ MeV/c^2. Similar results are found for the other channel.

[13]M. Aguilar-Benitez *et al.*, Phys. Lett. **170B**, 1 (1986).

[14]R. M. Baltrusaitis *et al.*, Phys. Rev. Lett. **52**, 2126 (1984).

[15]T. L. Trueman, Phys. Rev. D **18**, 3423 (1978); N. P. Chang and C. A. Nelson, Phys. Rev. D **20**, 2923 (1979).

[16]The value for a is obtained from a weighted average of the non-$\phi\phi$-background events below 2.4 GeV in both modes.

[17]The $\xi(2230)$ corresponds to the $X(2220)$ and the g_T's correspond to $f_2(2010)$, $f_2(2050)$, and $f_2(2340)$ in the Particle Data Group classification.

[18]R. Sinha, S. Okubo, and S. F. Tuan, Phys. Rev. D **35**, 952 (1987). In $J/\psi \to \gamma\rho\rho$ this prediction was found to be inconsistent with a limit determined by DM2 (see Ref. 5).

[19]D. P. Stanley and D. Robson, Phys. Rev. D **21**, 3180 (1980); S. Godfrey and N. Isgur, Phys. Rev. D **32**, 189 (1985).

[20]M. Chanowitz and S. Sharpe, Nucl. Phys. **B222**, 391 (1981).

[21]B. A. Li, in *Proceedings of the Tau/Charm Workshop* (SLAC Report No. SLAC-PUB-5007, 1989), p. 816; (private communication).

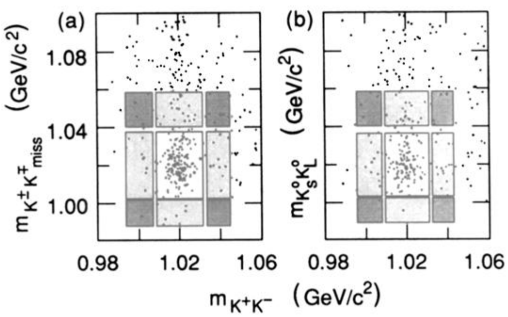

FIG. 1. Scatter plots for $J/\psi \rightarrow \gamma 4K$: (a) $m_{K^+K^-}$ vs $m_{K^\pm K^\mp_{miss}}$, plotting only the combination closest to the $\phi\phi$ overlap region; (b) $m_{K^+K^-}$ vs $m_{K^0_S K^0_L}$. Events in the shaded regions are used for background estimates.

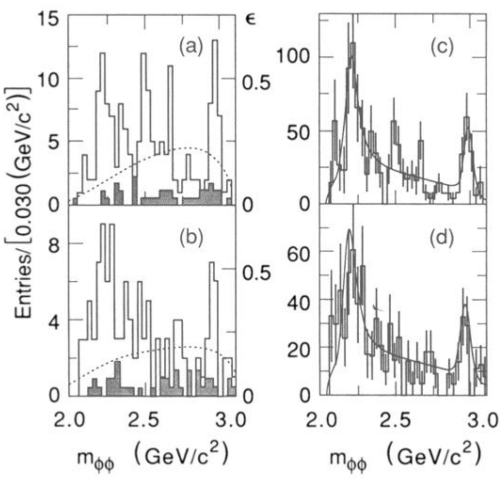

FIG. 2. The observed $\phi\phi$ invariant-mass spectra from (a) $J/\psi \rightarrow \gamma K^+K^-K^+K^-$ and (b) $J/\psi \rightarrow \gamma K^+K^-K_S^0K_L^0$; (c),(d) the corresponding $\phi\phi$ invariant-mass spectra after efficiency correction. Shaded histograms show background estimates; dashed curves show detection efficiencies denoted by ϵ; solid curves show fits described in the text.